

Conference Paper, Published Version

Bateman-Pinzon, Allen; Medina-Iglesias, Vicente; Guevara, Alex
Experimental Study of the Influence of Non-Hydrostatic
Pressure in Rip Rap Pier Protection

Verfügbar unter/Available at: <https://hdl.handle.net/20.500.11970/100275>

Vorgeschlagene Zitierweise/Suggested citation:

Bateman-Pinzon, Allen; Medina-Iglesias, Vicente; Guevara, Alex (2010): Experimental Study of the Influence of Non-Hydrostatic Pressure in Rip Rap Pier Protection. In: Burns, Susan E.; Bhatia, Shobha K.; Avila, Catherine M. C.; Hunt, Beatrice E. (Hg.): Proceedings 5th International Conference on Scour and Erosion (ICSE-5), November 7-10, 2010, San Francisco, USA. Reston, Va.: American Society of Civil Engineers. S. 639-648.

Standardnutzungsbedingungen/Terms of Use:

Die Dokumente in HENRY stehen unter der Creative Commons Lizenz CC BY 4.0, sofern keine abweichenden Nutzungsbedingungen getroffen wurden. Damit ist sowohl die kommerzielle Nutzung als auch das Teilen, die Weiterbearbeitung und Speicherung erlaubt. Das Verwenden und das Bearbeiten stehen unter der Bedingung der Namensnennung. Im Einzelfall kann eine restriktivere Lizenz gelten; dann gelten abweichend von den obigen Nutzungsbedingungen die in der dort genannten Lizenz gewährten Nutzungsrechte.

Documents in HENRY are made available under the Creative Commons License CC BY 4.0, if no other license is applicable. Under CC BY 4.0 commercial use and sharing, remixing, transforming, and building upon the material of the work is permitted. In some cases a different, more restrictive license may apply; if applicable the terms of the restrictive license will be binding.



Experimental Study of the Influence of Non-Hydrostatic Pressure in Rip Rap Pier Protection

Allen Bateman-Pinzon¹, Vicente Medina-Iglesias¹, Alex Guevara¹

Sediment Research Group (GITS-UPC) Technical University of Catalonia. Calle Gran Capitán s/n. 08034 Barcelona. Spain. Email: allen.bateman@gits.ws; vicente.medina@gits.ws

ABSTRACT

The non-hydrostatic pressure distribution is one of the main factors that affect the particles motion threshold around piers. The present paper focuses on the comparison of the motion threshold between circular-shaped and square-shaped piers under the influence of the non-hydrostatic pressure factor. A total of 30 runs were performed with different geometric dimensions and different Rip Rap diameter protection. The hydrostatic pressure factor distinguishes quite well between circular-shaped and square-shaped piers. Comparison with other authors has been made in order to extract some conclusions and confirm the experimental data. The non-hydrostatic pressure distribution on bed surfaces is very important to distinguish between different behaviors in sediment transport bed processes; local scour protection around piers is only an example. The main idea would be finding the threshold of motion of the Rip Rap around the circular-shaped and square-shaped base piers.

Keywords: Rip Rap, Pier Scour, Threshold of Motion

INTRODUCTION

Obstructions elements such as piers located in the middle of streams are responsible for the formation of local scour around thereof. Bridge-Piers are one of the most famous elements due to the impact on highways traffic flow and normal life when they fail; literally the bridge collapses and the traffic is interrupted. The present work relates to understanding the influence of the non-hydrostatic pressure distribution around piers as one of the most important parameters which affects the maximum depth of the local scour, (Bateman et al 2005).

Bridge piers and abutments collapsing frequently occurs around the world and is the main factor causing bridges to fall due to hydraulics and scour, in the U.S at least 90% of the times, Richardson et al. (1993). Protection of piers using Rip Rap is one of the principal actions carried out to avoid the collapse under storm conditions.

The present paper focuses on the threshold of the movement of particles located around the pier, being different due to the shape of the pier, -square or circular-, and to the influence of the non-hydrostatic pressure present around the pier.

All the experiments were performed at the Morphodynamic Laboratory of the Hydraulic, Marine and Environmental Department of the Technical University of Catalonia under the supervision of GITS-UPC(Sediment Transport Research Group).

Some theoretical aspects

In order to analyze the process describing the initial process of threshold of motion of particles around piers, the parameters can be classified as:

Parameters describing the fluid: The density (ρ) and the viscosity (ν) depend on the fluid temperature and salinity.

Parameters describing sediment: 50% by weight passing through the sieve size (D_{50}), the standard deviation of the sediment bed (σ), the density of the sediment (ρ_s) and the internal friction angle (ϕ).

Parameters describing the flow: Water depth(h), mean velocity(u), mean friction slope(S_f), mean slope of the stream(S_0), shear stress (τ_0) and non-hydrostatic pressure head increment ($\Delta P/\gamma$).

Parameters describing the obstacle: The shape and dimension (Circular with diameter(D) or Square with length size (D)), the orientation related to the flow direction (α).

Relation of the main authors whom work with Rip Rap protection in bridge piers

There are many authors since Shields fixed the basis of threshold of motion of particles. Indeed the first Rip Rap equation used is the relation between the dynamic fluid stress and the submerged weight of the sediment particle is the Shields relationship, (FHWA Hydraulic Engineering Circular, 1997). An expression of the same type was introduced by Isbash (1935) ((FHWA Hydraulic Engineering Circular, 1995), the change in the formulation was based on the equivalence of fluid stress to momentum flux. The equation explicitly presents now the velocity. The Maynard (1989) formula was the most extended one to evaluate the Rip Rap diameter protection. The equation is similar to Isbash equation, including the mean velocity of the fluid, but introducing a factor which depends on the sediment characteristics D_{30} .

In 1973 Neill proposed a dimensionless formula including the Froude number to an exponent of 2.5, but excluding the velocity, see Choi et al (2002). Also you can look for Bonasoundas (1973), Quazi Peterson (1973) Breusers et al. (1977), Parola C. (1993), Chiew (1995), Richardson et al. (1993), Yoon & Park (1997), Launchlan & Melville (2001), and finally Unger et al. (2006). All the formulae have the same type

of parameters, Froude number, sediment size ratio or standard deviation, the size of the pier and in general adjusting parameters. The most exhaustive formula is presented by Launchlan & Melville (2001) and can be expressed as:

$$\frac{D_{50}}{h} = K_y K_D K_C K_T K_S K_a Fr^2 \quad (1)$$

wherein, K_y is a parameter that includes the sediment depth Rip Rap protection with respect to the water depth, K_D is a parameter that includes the influence of the pier diameter, K_C is a factor relative to the protected area, K_T includes the effect of the protection depth, K_S corresponds to the influence of the pier shape, K_a is the alienation of the pier with respect to the flow direction. Launchlan & Melville (1999) describe several parameters which influence the Rip Rap protection, but which only fixed the K_y and K_C parameters.

Experimental Set Up

The Flume: To carry out the experiments, the flume from the Morphodynamic Laboratory of GITS-UPC was used; one of its devices consists in a flume having a 40 cm width and 60 cm height rectangular section and a total length of 9 meters. The discharge capacity goes from 250 cm³/s to 50 l/s controlled by two valves and two ultrasonic flowmeters. The downstream level was controlled by a mechanical slice gate locates at the end section of the flume.

Sediment characteristics: Four types of sediment size were used and were classified from big to small size with colours; white stones, black stones, gray stones, and gray filtered stones. Density and sediment size distribution can be seen in Table 2. The density was measured with a pycnometer and due to the uniform size of the stones, the mean diameter was measured with a Venier Caliper, at least one hundred stones were measured from a quarter sample methodology.

Experiment arrangement: A 10 cm gray stone base material ($D_{50}=7.34$ mm) was placed at the middle of the flume filling a length of 3m, as shown in Figure 1. The slope of the flume and sediment bed was 0°. The piers were placed one by one in the downstream at the 2/3 end part of the sediment bed.

Piers: Three circular-shaped and four square-shaped piers, for a total of 7 piers were used; the diameters of the circular piers were 1, 2 and 3 cm and the sides of the square-shaped ones were 1, 2, 3 and 4.2 cm.

Pressure measuring system: The pressure system consists of four water manometers strategically placed, the first one was placed 1 meter upstream from the front pier in order to control the normal pressure, the second one was placed in front of the pier and the third one was placed at the lateral side of the pier. The lateral manometer was placed at the point where the minimum pressure was predicted to

appear. The manometers were formed by two mm diameter plastic tubes and the water inside them was coloured with red ink to facilitate the visualization of the measurements.

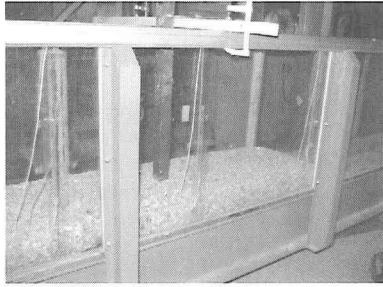


Figure 1. A photograph showing the experiment set up.

Discharge and water level measurements: Discharge measurements were carried out with an ultrasonic flowmeter and corroborated by a rectangular weir, and the water levels, upstream and downstream from the pier, were measured with a level meter.

Threshold of motion: The experiment purpose is to visually detect the threshold of motion of the particles surrounding the pier, as well as to precise the location where a displacement of stones is more susceptible to occur. The material was arranged at least in two layers around the pier covering an area more than three times the width of the pier.

The Rip-Rap movement was visually detected, when one or two stones were dragged by the flow stream; the threshold of the motion location was marked. In this case the discharge, pressure and water levels were measured. The discharge was increased by steps, firstly with the gate in a completely closed position, and then the gate was manually opened by steps, thus increasing the stress on the material until a movement has or has not been noticed. As soon as the range of discharges were accomplished, another pier and/or material was replaced, and the experiments was started again. Ninety experiments were established in order to detect the threshold of motion of the particles; six of them were discarded due to specific problems or due to a wrong procedure being carried out. The bigger problems were detected when small pier or sediment size begun to affect accuracy of measurements shown by data having the highest deviation.

A VORTEX ENERGY APPROACH.

The threshold of motion can be defined as the moment in which the work done by the fluid (vortex activity or stresses) exceeds the work done by gravity plus friction forces. It is possible to analyze the power of the fluid and gravity forces to

find a relationship between the parameters at the moment in which the threshold of motion occurs.

The power of the flow has to be equal to the rate of work done by the gravity in order to reach the threshold of motion. The power caused by gravity on the particle can be evaluated by multiplying the fall velocity of the particle times the submerged weight per unit mass.

$$P_g = (S_s - 1)g \cdot \omega_s \quad (1)$$

Wherein P_g is the work done by gravity forces per unit time and unit mass, S_s is the relative density of the bed sample, g is the gravity acceleration and ω_s is the fall velocity for a specific diameter. By definition the specific submerged weight is $R = S_s - 1$. The dimensions of equation (1) are L^2/T^3 .

The fall velocity, simply expressed, can be evaluated by the following expression:

$$\omega_s = \sqrt{\frac{4}{3} \frac{D}{C_D} Rg} \quad (2)$$

On the other hand some of the main reasons for sediment motion around the pier, and therefore the threshold of motion of the particles, are the horseshoe vortices formed in front of the pier. In Bateman et al. (2005) a relationship between the flow velocity and the power per unit mass contained in the vortex is:

$$\frac{1}{2} \frac{d(u^2)}{dt} = \frac{u^3}{\ell} \quad (3)$$

Batchelor (1953) expresses the kinetic energy velocity dissipation per unit mass of the vortex. Wherein, u is the mean approximation velocity and ℓ the integral length. Indeed the flow in the channel must have enough energy per unit time as to maintain the vortex activity. This is the main idea to relate the activity of the vortex with the sediment stability in the bed close to the pier. The length of the vortex has to be proportional to the depth of water in front of the pier, which is the depth of water in the approximation zone plus the excess of elevation due to the stagnancy of the flow in front the pier. That is:

$$\ell = \alpha (s_e + y_0) \quad (4)$$

Wherein S_e is the excess of depth of water in front of the pier and y_0 the approximation depth and α is a parameter to approximate the best vortex size, (see Bateman et al., 2005).

It is possible to define a parameter which compares the rate of work done by gravity forces with the vortex dissipation rate as:

$$\phi_p = \frac{d\left(\frac{1}{2}u^2\right)}{P_g} = \frac{u}{R\omega_s} F^2 \quad (5)$$

Wherein F is the Froude number evaluated with the velocity approximation and the depth of water in front of the pier. The parameter α has no relevance in this context and thus its value was assumed to be one. The relationship ϕ_p greatly depends on the correct determination of the velocity, due to its dependence on the cube of the velocity.

PRESSURE GRADIENT DETERMINATION

In order to evaluate the influence of the non-hydrostatic pressure distribution a couple of manometers were installed around the pier. The idea is to evaluate the pressure drop around the pier. As we do not know exactly where the pressure drop will be higher, we measure the pressure difference between the front (maximum pressure) and the side (minimum pressure). The measurement of the difference of pressure is done along a length l_m between those points. This gradient generates an internal flow inside the sediment pores; the internal flow exerts a force on the particle which is normal to the surface of the bed facilitating the threshold of motion of the particles. It is difficult to predict where will the force be bigger, unless a 3D internal and external coupled flow numerical model is applied. The length l_m between measures is used to evaluate the gradient from both points of measure.

Figure 2 shows a schematic view of the pier location and the points on which the pressure has been obtained. The pressure gradient is calculated as:

$$\frac{\partial P/\gamma}{\partial l} = \frac{(P_s - P_p)}{\gamma L_m} \quad (6)$$

P_s and P_p are the pressure measured at the surface of the test bed at the front and side of the pier respectively and γ is the water specific weight.

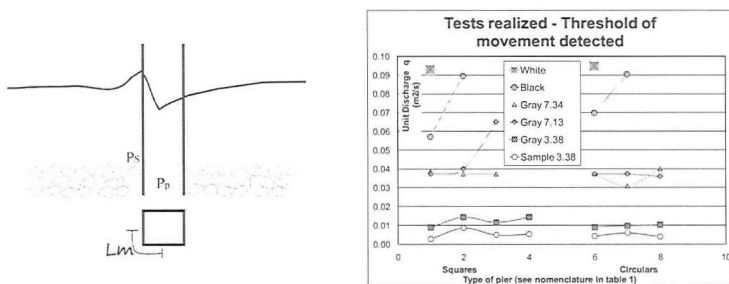


Figure 2. a) Description of the measurement pressure points. L_m is the length between the measurement pressure points P_p and P_s . b) Unit discharge at the threshold of motion for piers.

EXPERIMENTAL RESULTS

Table 1 shows the unit discharges in which the threshold of motion was detected. The data in parentheses shows no movement detected, the dash line shows non carried out experiments.

Table 1. Unit discharges in m^2/s at which threshold of motion was detected during the experiments.




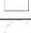



Type and width of pier number –shape-size-(cm)	White (16.9mm)	Black (13,32mm)	Grey (7.34 mm)	Grey (7.13mm)	Grey (3.38mm)	Sample (3.38mm)
1  4.2	[0,093]	0,057	0,039	0,037	0,009	0,003
2  3	-	[0,089]	0,037	0,040	0,014	0,009
3  2	-	-	0,037	0,065	0,011	0,005
4  1	-	-	-	-	0,014	0,005
6  4	[0,095]	0,070	0,037	0,037	0,009	0,004
7  3	-	[0,090]	0,031	0,037	0,010	0,006
8  2	-	-	0,040	0,036	0,010	0,004

Figure 3 shows the plots of the experiments of ϕ_p vs. the grain size and pier size ratio: D_g/D_p . The behavior of the circular- and square-shaped piers are clearly different. The lines show the conservative limit that can be used to make a design for pier protection.

In order to prove the consistency, a comparison with the main formulas was carried out. The method used was simply applying the formulae to the condition of the experimental data in order to obtain the D_{50} to protect the pier. Figure 6 shows the results upon applying the following formulae: Isbash, Richardson, Breusers, Bonasoundas and the implicitly presented formulation; more dispersion is detected compared with results shown in Figure 3.

Table 2 indicates the net pressure force due to the pressure gradient, and as can be seen it bears the same order of magnitude of the weight of the particle, depends on the type of experiment, but oscillates around from half to twice the weight of the particle. This quantity is relevant and capable for reducing the Shields parameter of the Rip Rap.

The most relevant results are given in Figure 3, wherein the variation of the pressure gradient respect to the relationship between sediment diameter and the pier width is shown. The data lies on two different paths; one for circular-shaped piers and the other for square-shaped piers. The white stones were so big and heavy that no movement thereof was caused during the experiments and therefore were not included in the table. From 90 equilibrated experiments only on 29 occasions a movement was detected. Figure 4 shows the points in which a stone has been seen moving. Note that all moving particles lie in the side part of the pier, except in the

square-shaped ones where some particles were moving in the back. The color graduation represents the relation between the grain size D_g with respect to the pier size D_p . The position at which the particles of sediment start to move are marked in a plan view in Figure 4.

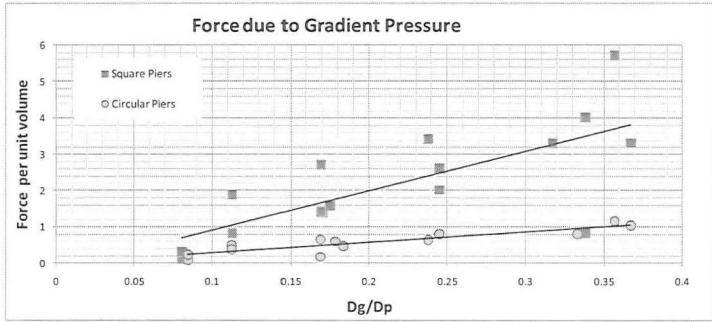


Figure 3. Force per unit volume due to the pressure gradient in square-shaped and circular-shaped piers to different grain size to pier size ratio.

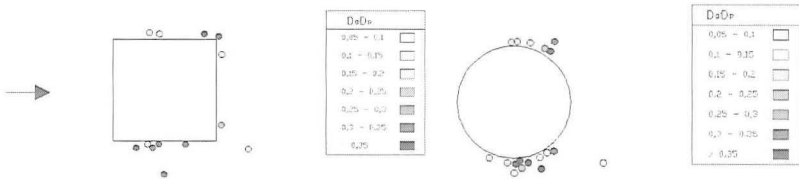


Figure 4. Points at which the particles start to move-colors are the ratio D_g/D_p . a) Square-shaped pier b) Circular-shaped pier

PROPOSED RELATIONSHIP

Once the pressure influence in both square-shaped and circular-shaped piers has been reached, we define the product of equation (5) and (6) and plot the results against the ratio between grain size and pier size diameter. This relationship is defined as:

$$\phi_p = \frac{u}{R\omega_s} F^2 \frac{\Delta P}{\gamma L_m} \tag{7}$$

Figure 5 shows the plots of the experiments of ϕ_p vs the grain size and pier size ratio: D_g/D_p . The behaviors of the circular- and square-shaped piers were clearly different. The lines show the conservative limit that can be used for designing pier protection.

In order to prove the consistency, a comparison between the main formulae was made. The method was carried out by simply applying the formulae to the conditions of the experimental data in order to obtain the D_{50} to protect the pier. Figure 6 shows the results of applying the following formulae: Isbash, Richardson,

Breusers, Bonasoundas and the formulation implicitly presented in (7); there was more dispersion detected compared with results shown in Figure 3.

Table 2. Results obtained from the pressure gradient in the experiments at the threshold of motion in square-shaped and circular-shaped piers.

Pier Type	Material	ρ_s	D_{50} (m)	Pressure increment (meters headwater)	Mean length L_m (m)	Pressure Gradient (m/m or (T/m ³))	Mean Particle Pressure Force (gr)	Particle Weight (gr)	Pressure Force over Weight (%)
Square 4.2	Grey	2.9	0.0071	0.029	0.021	1.38	0.262	0.556	47.1
Square 4.2	Grey	2.9	0.0073	0.033	0.021	1.57	0.325	0.607	53.6
Square 4.2	Black	3	0.0133	0.069	0.021	3.29	4.061	3.671	110.6
Square 3	Grey	2.9	0.0073	0.03	0.015	2.00	0.414	0.607	68.3
Square 3	Grey	2.9	0.0073	0.039	0.015	2.60	0.538	0.607	88.7
Square 3	sample	2.7	0.0034	0.012	0.015	0.80	0.016	0.054	30
Square 3	Grey	2.9	0.0071	0.051	0.015	3.40	0.645	0.556	116
Square 3	Grey	2.9	0.0034	0.028	0.015	1.87	0.038	0.059	63.7
Circular 4	Black	3	0.0133	0.037	0.047	0.79	0.97	3.671	26.4
Circular 4	Grey	2.9	0.0073	0.022	0.047	0.47	0.097	0.607	15.9
Circular 4	sample	2.7	0.0034	0.004	0.047	0.09	0.002	0.054	3.2
Circular 4	Grey	2.9	0.0071	0.028	0.047	0.59	0.113	0.556	20.3
Circular 4	Grey	2.9	0.0034	0.011	0.047	0.23	0.005	0.059	8
Circular3	Grey	2.9	0.0034	0.017	0.035	0.48	0.01	0.059	16.4
Circular3	sample	2.7	0.0034	0.013	0.035	0.37	0.007	0.054	13.8
Circular3	Grey	2.9	0.0071	0.022	0.035	0.62	0.118	0.556	21.2
Circular3	Grey	2.9	0.0073	0.028	0.035	0.79	0.164	0.607	27
Circular 2	Grey	2.9	0.0071	0.027	0.024	1.15	0.217	0.556	39.1
Circular 2	Grey	2.9	0.0034	0.015	0.024	0.64	0.013	0.059	21.7
Circular 2	sample	2.7	0.0034	0.004	0.024	0.17	0.003	0.054	6.4
Square 2	Grey	2.9	0.0073	0.033	0.01	3.30	0.683	0.607	112.6
Square 2	Grey	2.9	0.0071	0.057	0.01	5.70	1.082	0.556	194.5
Square 2	Grey	2.9	0.0034	0.027	0.01	2.70	0.055	0.059	92.2
Square 2	sample	2.7	0.0034	0.014	0.01	1.40	0.028	0.054	52.4
Square1	sample	2.7	0.0034	0.004	0.005	0.80	0.016	0.054	30
Square1	Grey	2.9	0.0034	0.02	0.005	4.00	0.081	0.059	136.5
Square 4.2	sample	2.7	0.0034	0.002	0.021	0.095	0.002	0.054	3.6
Square 4.2	Grey	2.9	0.0034	0.006	0.021	0.29	0.006	0.059	9.8
Circular 2	Grey	2.9	0.0073	0.024	0.024	1.02	0.211	0.607	34.8

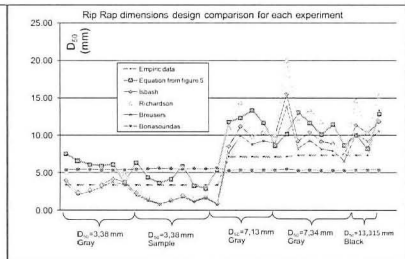
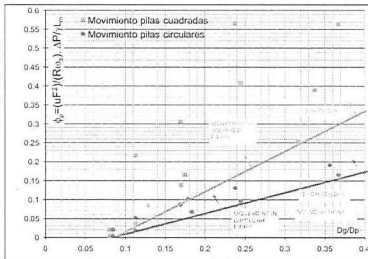


Figure 5. Plot of the equation (7) against the ratio of D_g to D_p . Figure 6. Application of the different formulae, Isbash, Richardson, Breusers, Bonasoundas and eq.(7).

CONCLUSION

The experiments that have been carried out at the Morphodynamic Laboratory of the Hydraulic, Marine and Environmental Engineering Department demonstrate the direct influence of the non-hydrostatic pressure distribution around the pier, and also that such situations are responsible in great measure for the threshold condition of the Rip Rap protection in piers. The application of the vortex power and work gravitational rate gives some physical explanation for the presence of the different parameters that will be present in the pier Rip Rap formulations.

BIBLIOGRAPHY

- Bateman, A. Fernández, Parker (2005), Morphodynamic model to predict temporal evolution of local scour in bridges piers. RCEM Urbana Champaign. Illinois 2005.
- Breusers, H. y Raudkivi, A.J. (1991), *Scouring*. IAHR Hydraulic Structures Design Manual. A.A. Balkema, Rotterdam, Holanda.
- Lauchlan, C.S. y Melville, B.W. (2001), *Riprap protection at bridge piers*. Journal of Hydraulic Engineering, Vol. 127 n°5, Mayo.
- Richardson, E.V., Harrison, L.J., Richardson J.r., y Davies, S. R. (1993), *Evaluating scour at bridges*. Publ. FHWA-IP-90-017, Federal Highway Administration, Washington, D.C.
- Stephen T. Maynard, James F. Ruff Steven R. Abt (1989), *Riprap design*. ASCE Journal of Hydraulic Engineering, Vol. 115 n° 7, Julio.
- S.V. Isbash. 1936 "Construction of Dams by Depositing Rock in Running Water," Communication No. 3, Second Congress on Large Dams, Washington, DC.
- FHWA-HI-97-030. 1997. HEC-23 <http://www.fhwa.dot.gov/engineering/hydraulics/pubs/hec/hec23.pdf>.
- Breusers, H. y Raudkivi, A.J. (1991), *Scouring*. IAHR Hydraulic Structures Design Manual. A.A. Balkema, Rotterdam, Holanda.
- Chiew, Y.M. (1995), *Mechanics of riprap failure at bridge piers*. ASCE Journal of Hydraulic Engineering, Vol. 121 n° 9, Septiembre.
- Choi, G.W. et al. (2002), Riprap equation for protecting the local scour at bridge piers. Journal of Korea Water Resources Association, Vol. 37 n°6.
- Isbash, S. V. 1936. "Construction of Dams by Depositing Rock in Running Water," Transaction, Second Congress on Large Dams, Vol 5, pp 123-126.
- Maynard S.T. (1988) "Stable Rip Rap Size for open channel Flows" tech. Rep. HL 884-4 US Army Engineering Waterways Experiment Station, Vicksburg Miss.
- Parola, A.C. (1993), Stability of riprap at bridge piers. Journal of Hydraulic Engineering, Vol. 119 n°10, Octubre.
- Richardson, E.V., Harrison, L.J., Richardson J.r., y Davies, S. R. (1993), *Evaluating scour at bridges*. Publ. FHWA-IP-90-017, Federal Highway Administration, Washington, D.C.
- Unger, J. y Hager, W.H. (2006), Riprap failure at circular bridge piers. ASCE Journal of Hydraulic Engineering, Vol. 132 n°4, Abril.
- Yoon, T.H. y Park, K. (2001), Effects of nonuniform bridge piers on riprap scour countermeasures. Proc. of 29th Congress of Int. Assoc. for Hydraulic Research.